Platinum(II) compounds with chelating ligands based on pyridine and pyrimidine: synthesis, characterizations, DFT calculations, cytotoxic assays and binding to a DNA model base

Roy, S.; Westmaas, J.A.; Buda, F.; Reedijk, J.

Journal of Inorganic Biochemistry 103 (2009) 1278–1287

Contents lists available at ScienceDirect

Journal of Inorganic Biochemistry

journal homepage: www.elsevier.com/locate/jinorgbio

Platinum(II) compounds with chelating ligands based on pyridine and pyrimidine: Synthesis, characterizations, DFT calculations, cytotoxic assays and binding to a DNA model base

Sudeshna Roy, Joyce A. Westmaas, Francesco Buda, Jan Reedijk *

Leiden Institute of Chemistry, Leiden University P.O. Box 9502, 2300 RA Leiden, The Netherlands

ARTICLE INFO

Article history:
Received 17 April 2009
Received in revised form 30 June 2009
Accepted 6 July 2009
Available online 4 August 2009

Keywords:
Platinum
Flexible amines
Antitumor
DFT
DNA model base
Time-dependent NMR
Cytotoxicity *in vitro*

ABSTRACT

Two chelating ligands based on secondary amines have been selected to prepare four new Pt(II) compounds. The ligands bis(pyridine-2-yl)amine, abbreviated **dpa**, and bis(pyrimidine-2-yl)amine, abbreviated **dipm**, are chosen to design a rigid chelating motif to allow the study of subtle differences in electronic properties and hydrogen bonding ability. Different carrier ligands (i.e. chloride and ammine) have also been introduced to allow a study of structure–activity relationships. Two of the four compounds are cisplatin analogues, whereas the other two are cationic and coordinatively saturated compounds. The four synthesized and characterized compounds are $[Pt(dpa)Cl_2]$, $[Pt(dpa)(NH_3)_2](NO_3)_2$, $[Pt(dipm)Cl_2]$ and $[Pt(dipm)(NH_3)_2](NO_3)_2$ with code numbers **C1**–**C4**. The spatial structures of all these compounds have also been optimized using DFT (density functional theory) calculations. The cytotoxicity of these compounds has been investigated in seven human tumor cell lines using the SRB (sulforhodamine B) assay. The most promising antitumor active compound appears to be **C3**, $[Pt(dipm)Cl_2]$. Two water-soluble compounds, **C2** and **C4** exhibit selective activity in EVSA-T cell line. In addition, the reaction of the cisplatin analogues with the model base 9-ethylguanine has been followed by proton and platinum NMR spectroscopy.

1. Introduction

The serendipitous discovery of cisplatin is generally considered to be a break-through in cancer treatment [1–3]. In the subsequent years it has been demonstrated that the combination of transition metals with appropriate ligands can lead to clinically-approved anticancer metallodrugs (like carboplatin, oxaliplatin, satraplatin), others like picoplatin, NAMI-A are still in clinical trials [2–5]. In this fertile field three main approaches to design new drugs are currently observed: (1) direct cisplatin analogues or modifications (2) use of other metals than platinum and (3) combination of known, active organic drugs with metal compounds. In general the aim of much new research is primarily focused on more efficient orally administrable drugs with minimum side toxic effects and on drugs with cisplatin-resistance, or multidrug resistance surpassing properties. To reach that target, some key characteristics of the metallodrugs are ideally required [6,7].

The generally accepted mechanism for the antitumor activity of cisplatin is the intrastrand DNA lesion. Activated cisplatin after hydrolysis of the chloride ligands coordinates to genomic DNA (purine bases, preferably guanine) thereby generating a kink in the helix [8,9]. On the other hand, other non-metallic antitumor drugs, like doxorubicin and daunomycin, are known to act by intercalating between the base pairs of DNA [10]. These compounds inhibit cell growth by mainly two pathways, (a) poisoning *Topoisomerase I* and *II*, which inhibits replication and (b) poisoning RNA polymerase which inhibits transcription. Therefore, bringing the best of these two facets together, i.e. combining coordination binding and intercalation in a single molecule could possibly lead to the generation of a new class of antitumor drugs.

The molecular structures of two chosen ligands with metal binding sites and H-bonding properties are depicted in Fig. 1. The ligand **dpa** [bis(pyridine-2-yl)amine] acts as a flexible chelating ligand by virtue of the central, non-coordinating, secondary amine moiety and contains only a solitary H-bond donor. Another recently reported ligand [11], **dipm** [bis(pyrimidine-2-yl)amine] has been selected for coordination to platinum, which can interestingly form a linear acceptor–donor–acceptor array of hydrogen bonds (as shown in Fig. 1) even after metal chelation. After coordination to platinum, both the ligands result in open book structure. In spite of these slightly puckered structures, these compounds possibly exert partial intercalation using chelating ligand (dpa or dipm) surface. Additionally the monodentate chloride (prone to

* Corresponding author.
E-mail address: reedijk@chem.leidenuniv.nl (J. Reedijk).

0162-0134/$ - see front matter © 2009 Elsevier Inc. All rights reserved.
doi:10.1016/j.jinorgbio.2009.07.004

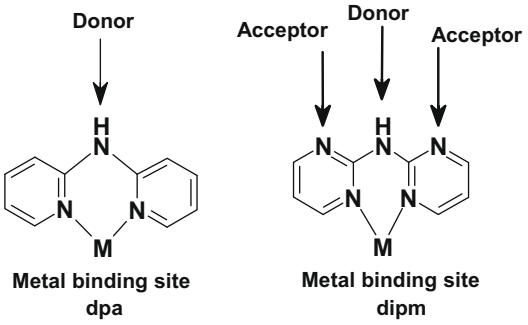

Fig. 1. Hydrogen-bond acceptor and donor sites in ligands **dpa** and **dipm** after chelation to a metal.

facile solvolysis) or ammine (render additional stability *via* hydrogen bonding) ligands carry out the initial role of attraction towards DNA. Thus the strategy of combining coordination and partial intercalation has been carried out.

In some recent articles **dpa** is reported [12–14] when coordinated with platinum or palladium with only very brief cytotoxicity tests. The compound, Pt(dpa)Cl_2 ,**C1**, has been reproduced for detailed biological experiments and DNA binding. A new cationic analogue, diammine(2,2′-dipyridine-2-ylamine)platinum(II) nitrate; [Pt(dpa)$(NH_3)_2$]$(NO_3)_2$, **C2**, has also been synthesized for comparison. This highly water-soluble compound overcomes the poor aqueous solubility problem of **C1**. The ligand **dipm** has also been studied in the literature, but mainly for structural studies with Cu [15,16]. So two new compounds dichlorido(2,2′-dipyrimidine-2-ylamine)platinum(II), [Pt(dipm)Cl_2], **C3** and diammine(2,2′-dipyrimidine-2-ylamine)platinum(II) nitrate, [Pt(dipm)$(NH_3)_2$] $(NO_3)_2$], **C4**, have been synthesized using **dipm** as carrier ligand. **C3** can be seen as a cisplatin analogue and **C4** is cationic and highly soluble with coordinatively saturated Pt(II) center. This series of four compounds was used for studying and comparing of (a) the effect of slight variation of the bidentate ligands, **dpa** and **dipm** and (b) neutral and cationic platinum compounds in their mode of action. Molecular structures of these four Pt(II) compounds are schematically shown in Fig. 2.

In this paper we report the *in vitro* cytotoxicity study of the four compounds in seven human tumor cell lines and the reactivity of the Pt(dpa) and Pt(dipm) units with the DNA model base 9-ethylgyanine. Using DFT (density functional theory) calculations the structures of all four compounds (**C1–C4**) have been optimized and their structures will be presented below. This calculation is significant to predict and explain the mode of interaction with biomolecules. A subsequent paper will deal with the study of the DNA and protein interactions of these four compounds [17].

2. Experimental

2.1. Materials

2-Chloropyrimidine was obtained from Acros Organics (The Netherlands). Potassium carbonate was purchased from Merck (Germany). Anhydrous $MgSO_4$ and *N,N*-diisopropylethylamine (dipea) were received from Fluka (The Netherlands). **dpa**, 9-ethylguanine (9-EtG), 2-aminopyrimidine and deuterated solvents for NMR were obtained from Sigma Aldrich B.V. (The Netherlands) and used directly as received. The starting material, K_2PtCl_4 was received as a generous loan from Johnson & Matthey (Reading, UK). Cisplatin was synthesized following a reported route [18]. Another platinum precursor, *cis*-[Pt(dmso)$_2Cl_2$] was synthesized following the reported synthetic procedure [19]. The ligand **dipm**, bis-(pyrimidine-2-yl)amine, was synthesized following a reported synthetic route [11] with some modifications and described in detail in Section 2.6. The solvents used for synthesis were purchased from Biosolve (AR grade, The Netherlands) and were used without further purifications.

2.2. Cell types and chemicals

The seven tumor cell lines used for this study are of the following origin: MCF7 (breast cancer (ER)+/(PgR)+), EVSA-T (breast cancer (ER)-/(PgR)-), WIDR (colon cancer), IGROV (ovarian cancer), M19-MEL (melanoma), A498 (renal cancer), H226 (non-small cell lung cancer). The medium [RMPI (Roswell memorial park institute)-1640] and 10% fetal calf serum were purchased from Gibco, Invitrogen, Paisley Scotland. Penicillin, streptomycin, SRB (sulforhodamine B) and dmso were received from Sigma, St. Louis, MO, USA and PBS (phosphate buffered saline) was obtained from NPMI B.V. Emmer-Compascum, The Netherlands. Carboplatin, Oxaliplatin and *R,R*-[Pt(dach)Cl_2] were purchased from Sigma Aldrich B.V. (The Netherlands).

2.3. Nuclear magnetic resonance spectroscopy

One- and two-dimensional NMR spectra were recorded on a Bruker DPX 300 MHz spectrometer at room temperature (21 °C), or at physiological temperature (37 °C). The solvents used were dmso-d_6, dmf-d_7, D_2O or a mixture of these solvents. The ^{195}Pt NMR spectra were referenced to an external standard, K_2PtCl_4 in D_2O ($\delta = -1614$ ppm). For the time-dependent one-dimensional serial studies spectra were collected with 48 scans and 15 min waiting time for a 24 h measurement. All data have been processed with the software packages XWIN-NMR and XWIN-PLOT [20].

2.4. Electrospray ionization mass spectrometry (ESI-MS)

ESI-MS measurements were carried out with a Thermo Finnigan Aqa mass detector. With the HPLC equipment 10 μL of the sample was introduced into the detector. Different solvents were used [methanol: water = 80:20 (v/v) or water] with a flow of 0.2 mL/min. Samples were measured in the positive mode using an ionizations voltage of 3 kV and a detector voltage of 20 mV with a probe temperature of 27 °C. The scanning range was m/z = 100–1400. For **C1** and **C3**, the dmso stock solution was directly infused in the instrument.

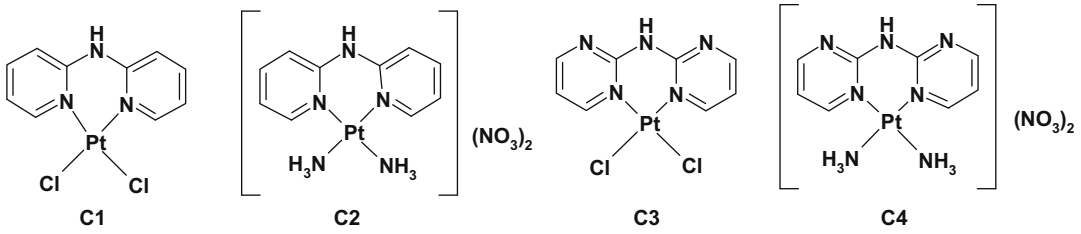

Fig. 2. Molecular structures of the four platinum compounds (**C1–C4**).

2.5. Elemental analysis

Elemental analysis of the samples was performed in a Perkin Elmer Series II CHNS/O Analyser 2400. Typically 2–2.2 mg of sample was used for C, H, N and S analysis. All measurements were performed in duplicate and the average value is reported.

2.6. Chemical syntheses

2.6.1. ***dipm***: *bis(pyrimidine-2-yl)amine*

The used synthetic route has been modified slightly from that reported in the literature [11]. The starting products dipea (37.1 g, 0.287 mol), 2-aminopyrimidine (10 g, 0.105 mol) and 2-chloropyrimidine (16.7 g, 0.105 mol) were mixed together and refluxed for 60 h. The reaction mixture was cooled down to room temperature and the excess of dipea was decanted. The residual brown paste was redissolved in 200 mL of boiling water and the aqueous layer was extracted several times with dichloromethane. The organic phase was collected, dried over anhydrous $MgSO_4$ and finally evaporated under reduced pressure to yield a yellow solid. The crude ligand was recrystallized from water. Yield of the recrystallized ligand (light brown needles) was 60%.

2.6.2. ***C1***: *cis-dichlorido(2,2′-dipyridine-2-ylamine)platinum(II), cis-[Pt(dpa)Cl$_2$]*

This compound had already been reported by others [12,13] and the synthesis has been reproduced, but with some additional characterizations. Two different platinum starting materials have been used in an attempt to optimize the yield and recipe.

2.6.2.1. Method 1: from cis-[Pt(dmso)$_2$Cl$_2$]. The starting material, *cis*-[Pt(dmso)$_2$Cl$_2$] (0.010 g, 0.24 mmol) was dissolved in a minimum amount of dmso. A solution of **dpa** (0.040 g, 0.24 mmol) in a minimum amount of dmso was added. The yellow solution was stirred for 3 days at room temperature. Removal of solvent under reduced pressure yielded a yellow colored product (0.087 g, 83%).

2.6.2.2. Method 2: from K_2PtCl_4. The platinum precursor, K_2PtCl_4 (0.050 g, 0.12 mmol) was dissolved in 6 mL of water and a solution of **dpa** (0.020 g, 0.12 mmol) in 2 mL ethanol was added dropwise. The mixture was stirred overnight at 50 °C. A yellow precipitate had formed, which was filtered off and washed with ice-cold water and acetone. The yield after purification was found to be 0.018 g (34%).

2.6.3. ***C2***: *cis-diammine(2,2′-dipyridine-2-ylamine)platinum(II) nitrate, cis-[Pt(NH$_3$)$_2$(dpa)](NO$_3$)$_2$*

Cis-[Pt(NH$_3$)$_2$Cl$_2$] (0.050 g, 0.167 mmol) was dissolved in 2 mL of dmf. A solution of silver nitrate (0.056 g, 0.333 mmol) in 1 mL of dmf was added and the mixture was stirred overnight at room temperature in the dark. The precipitate was filtered off and **dpa** (0.028 g, 0.167 mmol) was added to the filtrate. The mixture was stirred for 4 days at room temperature in the dark. A small amount of a greenish precipitate (mostly polymer, or Magnus-salt like ionic aggregates [21]) was filtered off. Diethyl ether was added slowly to the filtrate to precipitate the buff-white product. The product was washed with a small amount of cold water and the product (0.041 g, 47%) was air dried.

2.6.4. ***C3***: *cis-dichlorido(2,2′-dipyridine-2-ylamine)platinum(II), cis-[Pt(dipm)Cl$_2$]*

This compound was synthesized using *cis*-[Pt(dmso)$_2$Cl$_2$] (prepared as reported in literature [19]) as the starting material. The *cis*-[Pt(dmso)$_2$Cl$_2$] (0.050 g, 0.118 mmol) was dissolved in a minimum amount (~4 ml) of dmso. A solution of **dipm** (0.020 g, 0.118 mmol) in a minimum amount of dmso (~3 ml) was added dropwise to the platinum solution. The yellow solution was stirred for 3 days at 50 °C in the dark. Slow addition of diethyl ether to the reaction mixture initiated precipitation of the product. The yellow precipitate was dried in air to yield 0.032 g (63%) of product.

2.6.5. ***C4***: *cis-diammine(2,2′-dipyrimidine-2-ylamine)platinum(II) nitrate, cis-[Pt(NH$_3$)$_2$(dipm)] (NO$_3$)$_2$*

An amount of *cis*-[Pt(NH$_3$)$_2$Cl$_2$] (0.050 g, 0.167 mmol) was dissolved in a minimum amount of dmf in the dark. A solution of silver nitrate (0.056 g, 0.333 mmol) in 1 mL dmf was added and the mixture was stirred overnight at room temperature. The precipitate was filtered off and **dipm** (0.028 g, 0.167 mmol) was added to the filtrate. The mixture was stirred for two days at room temperature. Diethyl ether was added to precipitate the pale yellow product with a yield of 0.043 g (64%).

2.7. Analysis

2.7.1. ***dipm***

The ligand was characterized by ^{1}H and ^{13}C experiments and matched with reported values [11]. Elemental analysis (%) for $C_8H_7N_5{\cdot}2H_2O$ (water from recrystallization): expt. (calcd.) C 45.55 (45.93), N 33.58 (33.48), H 5.54 (5.30). ESI-MS measurements of a freshly prepared solution of recrystallized **dipm** in methanol show cationic peaks at m/z = 196 and 228, which corresponds to Na + **dipm** and Na + **dipm** + CH_3OH species, respectively.

2.7.2. ***C1***

The synthetic routes from different starting Pt-precursors yield the same platinum compound as confirmed by several analytical techniques, however, the yields are different. The ^{1}H and ^{195}Pt NMR in dmso-d_6 characterized the desired product. The one-dimensional proton NMR shows the following peaks with the numbering described in Fig. 7. The assignments for ^{1}H NMR (in dmso-d_6, s = singlet, d = doublet, t = triplet) δ (ppm): 11.0 (s, 1H; H7), 8.7 (d, 2H; H2,2′), 7.9 (t, 2H; H3,3′), 7.2 (d, 2H, H5,5′), 7.1 ppm (t, 2H, H4,4′). The ^{195}Pt (in dmso-d_6) spectrum shows a peak at δ −2094 ppm, which corresponds to PtN_2Cl_2 environment [22,23]. ESI-MS of a freshly prepared solution (in dmso and direct infusion to instrument without further dilution), shows the prominent peak at 479.6, which corresponds to the species, [Pt(dpa)Cl(dmso)]$^+$ with a typical platinum isotopic pattern. Elemental analysis (%) for $PtC_{10}H_9N_3Cl_2$: expt. (calcd.) C 26.56 (27.47), N 9.30 (9.61), H 2.16 (2.07). The percentage of carbon is little higher than the theoretical value but the value is reported as obtained. The spectroscopy did not show unusual features, so the difference in values is ascribed to experimental errors, which is not uncommon for this heavy-metal containing compound.

2.7.3. ***C2***

The ^{1}H and ^{195}Pt NMR were recorded in D_2O and show characteristic peaks from **dpa** coordination. ^{1}H NMR (D_2O) (ppm): δ 8.1 (d, 2H; H2,2′), 7.8 (t, 2H; H3,3′), 7.2 (d, 2H; H5,5′), 7.0 (t, 2H, H4,4′), 4.6 ppm (s, 6H, H8,8′). The ^{195}Pt shows peak at δ = −2584 ppm, corresponding to a PtN_4 environment [22,23]. A fresh solution in water (elution with water only) gives rise to the peak at m/z = 401, corresponding to the species, [Pt(dpa)(NH$_3$)(OH)]$^+$ which possibly is formed during measurement. Elemental analysis (%) for $PtC_{10}H_{15}N_7O_6$: expt. (calcd.) C 22.77 (22.91), N 18.41 (18.70), H 2.94 (2.88).

2.7.4. ***C3***

The ^{1}H NMR spectrum in dmf-d_7 shows small shifts compared to the free ligand. ^{1}H NMR (dmf-d_7) δ (ppm): 10.2 (s, 1H; H7), 9.3 (d, 2H; H2,2′), 8.8 (d, 2H; H4,4′), 7.3 (t, 2H; H3,3′). The ^{195}Pt spectrum (in dmf-d_7) shows a peak at δ −2049 ppm, which corre-

sponds to a PtN_2Cl_2 environment [22,23]. MS from a fresh solution (solution made in dmso and direct infusion the spectrometer) shows the major peak at $m/z = 481$, which corresponds to the $[Pt(dipm)Cl(dmso)]^+$ species with a typical platinum isotopic pattern. Elemental analysis (%) for $PtC_8H_7N_5Cl_2$: expt. (calcd.) C 21.33 (21.88), N 14.80 (15.95), H 1.84 (1.61). The percentage of nitrogen is little higher than the theoretical value but the value is reported as obtained. The spectroscopy did not show unusual features, so the difference in values is ascribed to experimental errors, which is not uncommon for this heavy-metal containing compound.

2.7.5. *C4*

The ^1H NMR in dmso-d_6 shows small shifts compared to free ligand and the peak positions are given as ^1H NMR δ (ppm): 10.2 (s, 1H; H7), 8.9 (d, 2H; H2,2′), 8.7 (d, 2H; H4,4′), 7.4 (t, 2H; H3,3′), 4.8 (s, 6H; H8,8′). The ^{195}Pt NMR in the same solvent shows a single peak at δ −2504 ppm, which corresponds to a PtN_4 coordination motif [22,23]. MS (elution with water) shows a major peak at $m/z = 401$, which corresponds to $[Pt(dipm)(NH_3)(OH)]^+$ species (which possibly is originated during measurement) with a typical platinum isotopic pattern. Elemental analysis (%) for $PtC_8H_{13}N_9O_6$: expt. (calcd.) C 18.26 (18.26), N 23.69 (23.95), H 2.42 (2.49).

2.8. Computational details

Density functional theory (DFT) calculations have been performed with the Amsterdam density functional (ADF) program [24–26]. The BLYP [27,28] exchange–correlation functional and applied relativistic corrections within the zero order regular approximation (ZORA) [29] for all the elements have been used. The relativistic corrections are particularly relevant for heavy elements, such as Pt. In the ADF code the electronic orbitals are written in terms of Slater-type functions (STO). The ZORA formalism requires specially adapted basis sets, and the relativistic basis set ZORA/TZ2P (triple-zeta including two sets of polarization functions) was used. The ZORA formalism has been used also for the geometry optimization of all the compounds. The effect of the relativistic corrections is significant and the agreement with experimental data for the **C1**, $[Pt(dpa)Cl_2]$ compound improves considerably [12,13]. In particular for the Pt–Cl (Pt–N) distance, an error of 5% (9%) observed without ZORA, decreases to 2% (3%) including ZORA.

2.9. DNA model-base studies

The commonly used [30] 9-ethylguanine was applied as a model nucleobase to follow the coordination interaction with the platinum compounds, **C1** and **C3**. **C2** and **C4** are coordinatively saturated without any easily labile ligands and were not studied. One-dimensional NMR and ESI-MS spectra were recorded over time. Different molar equivalents (platinum compound: model base = 1:1 or 1:4) of model base were added to the compound solution and allowed to react in deuterated solvent over 12 h. The fastest reactions occur when the ratio of platinum compound: model base was used as 1:4. The volume of the solvent was kept constant at 700 μL and the Pt-sample concentration was 5 mM for all experiments. Reactions were followed by NMR spectroscopy over 7 days. To follow the changes around the platinum coordination sphere, ^{195}Pt spectra were recorded over time to follow any changes in the Pt-coordination sphere. ESI-MS spectra were recorded over specific time intervals.

2.10. In vitro cytotoxicity assay

The cytotoxicity of the platinum compounds (**C1–C4**) and the corresponding free ligands (**dpa–dipm**) was analyzed using the microculture sulforhodamine B (SRB) test [31]. This colorimetric assay was carried out generously by TEVA-Pharmachemie (Haarlem, The Netherlands). Human tumor cell lines used were WIDR, IGROV, M19 MEL, A498 and H226 (which belong to the currently used anticancer screening panel of the National Cancer Institute, USA), MCF-7 (contains estrogen and progesterone receptors) and EVSA-T (lacks both hormone receptors). All cell lines were maintained in a continuous logarithmic culture in RMPI-1640 medium with HEPES (*4-(2-hydroxyethyl)-1-piperazineethanesulfonic acid*) and phenol red. The medium was supplemented with 10% FCS, penicillin (100 IU/mL) and streptomycin (100 μg/mL). The cells were mildly trypsinized for passage and for use in the experiments. Briefly, the experiments were started on day 0. Flat-bottomed 96-welled microtiter plates (*Cellstar, Greiner Bio-one*) were used to plate 150 μL of trypsinized tumor cells (1500–2000 cells/well). The plates were then preincubated for 48 h at 37 °C in 5% CO_2 atmosphere to allow cells to adhere. On day 2, a threefold dilution sequence of 10 steps was made in full medium starting from 0.25 mg/mL stock solution. Each dilution was used in quadruplicate by adding 50 μL to a column of four wells. This stepwise addition from low to high concentrations of sample reached the highest concentration of 0.062 mg/mL in column 12. In column 1, only full medium was added to diminish interfering evaporation and column 2 was used for a blank in each cell plate. The pictorial presentation of the cell plates is shown in Fig. S1.

After the termination of incubation on the 7th day, cells were fixed with 10% TCA in PBS and incubated at 4 °C for 1 h. After three washings with water the cells were stained for 15 min with 0.4% SRB in 1% acetic acid. Subsequently, cells were washed with 1% acetic acid, air-dried and the bound stain was dissolved in 150 μL 10 mM Tris-base (unbuffered). The value of A_{540} was assessed using an automated microplate reader (Labsystems Multiskan MS). Data were used for concentration–response curves and ID_{50} values using Deltasoft 3 software (Biometallics Inc., Princeton, NJ, USA). The IC_{50} values were obtained after proper unit conversion of the ID_{50} values. The so-obtained IC_{50} values correspond to the concentration of the drug required for 50% inhibition of cell growth.

3. Results and discussion

3.1. General comments

In this study, four new platinum compounds with differences in structure and property (both chemically and electronically) are reported. The aim has been to investigate their bio-physical properties and *in vitro* cytostatic activities. In addition to the chelating ligands, these compounds carry relatively labile chloride ligands (for **C1** and **C3**), or non-leaving hydrogen-bond donor ammine groups (**C2** and **C4**). The changes in these ancillary ligands may help to modify the chemical properties, which undoubtedly will be reflected in their interaction with different biological targets. These results are useful to correlate the biophysical studies with *in vitro* cytotoxicity. The flexibility of the aromatic ligands opens up the possibility of new ligand design, which appears promising to develop new anticancer Pt-drugs.

3.2. Syntheses and characterizations

The synthesis of **dipm** and the platinum compounds (**C1–C4**) went straightforward. For compounds **C1** and **C3**, the metal precursor (K_2PtCl_4 or *cis*-$[Pt(dmso)_2Cl_2]$) was used to react with 1 M equivalent of the ligands in different solvents (see experimental part in 2.6) and the products are obtained as yellow precipitates. For compounds **C2** and **C4**, *cis*-$[PtCl_2(NH_3)_2]$ is used as a precursor.

Recrystallized cisplatin is activated by using 2 M equivalent of $AgNO_3$, followed by ligand addition. The desired products are obtained by thorough washing with ether (and acetone, for **C2**) and drying in air.

The one-dimensional (^1H and ^{195}Pt) and two-dimensional (COSY) NMR spectroscopic data provide unambiguous identification of the expected peaks. As a solvent, dmso-d_6 or dmf-d_7 is used for **C1** and **C3**, whereas the high aqueous solubility of **C2** and **C4** allows recording the NMR spectra in D_2O.

The ESI-MS analysis provides evidence for the major species present in solution. For **C1** and **C3**, direct infusion to the spectrometer shows the cationic species as a major peak, with one chloride substituted for dmso (solvent). For **C2** and **C4**, the major ion species assigned to, are possibly originated after dissociation of a ligand ammine, along with some minor dissociation species. For elemental analysis the data are within the range when compared to the calculated weight percentage of the elements. Unfortunately, suitable crystals for X-ray diffraction were not obtained; therefore the structures were optimized using DFT calculations (see below).

3.3. Optimized structures by DFT calculation

As no single crystal for X-ray diffraction studies could be obtained the structures of the compounds **C1–C4** have been optimized using DFT in vacuum and are shown in Figs. 3–6 together with the electronic HOMO (highest occupied molecular orbital)-LUMO (lowest unoccupied molecular orbital) pictures. A direct comparison with experimental data appeared possible for compound **C1**, whose structure had been reported in the literature [12,13]. Thus the structure of **C1** has been used as a starting and reference structure to generate the initial models for the remaining compounds [13]. The comparison of some structure details for **C1**, calculated and observed, is given in Table 1, showing a very good agreement indeed.

The calculated structure for **C1** is in good agreement with the available crystal structure data (*vide* Table 1), both in terms of bond angles and bond lengths. DFT is known [32,33] to slightly overestimate bond lengths by approximately 2% on average. Any crystal packing [13] effects are neglected in the model.

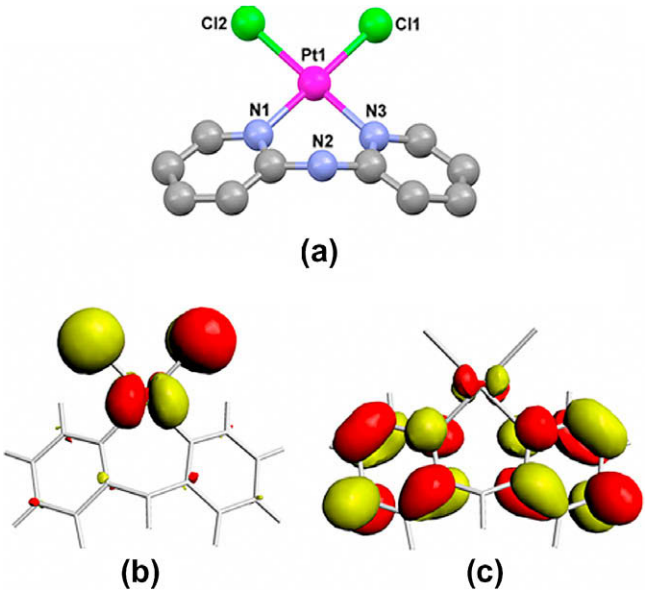

Fig. 3. Energy minimized structure of **C1** (a), (b) HOMO and (c) LUMO. The red (dark) and green (light) isosurfaces correspond to positive and negative isosurface values (±0.03), respectively. (For interpretation of the references to colour in this figure legend, the reader is referred to the web version of this article.)

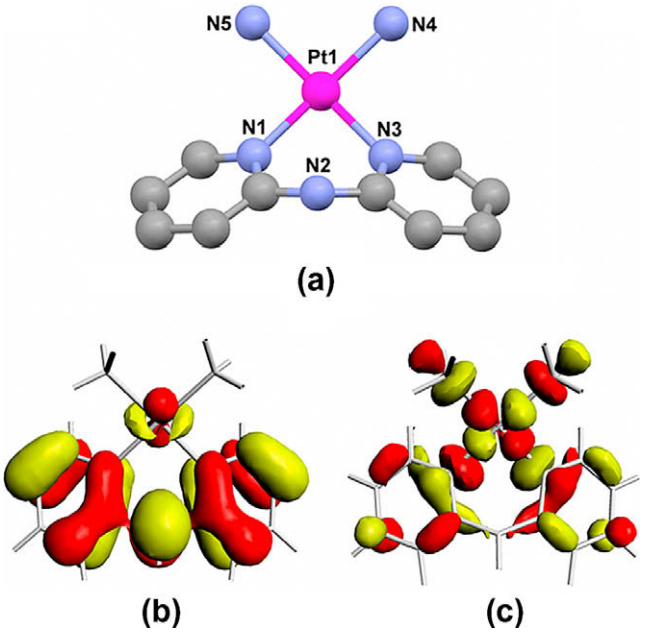

Fig. 4. Energy minimized structure of **C2** (a), (b) HOMO and (c) LUMO. The red (dark) and green (light) isosurfaces correspond to positive and negative isosurface values (±0.03), respectively. (For interpretation of the references to colour in this figure legend, the reader is referred to the web version of this article.)

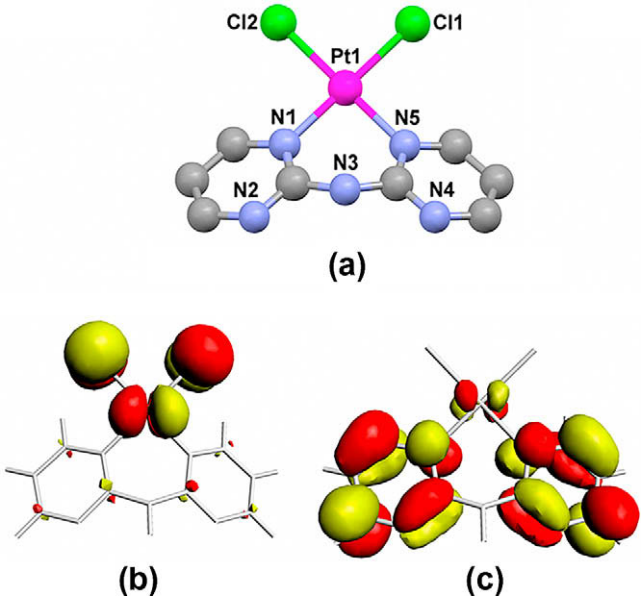

Fig. 5. Energy minimized structure of **C3** (a), (b) HOMO and (c) LUMO. The red (dark) and green (light) isosurfaces correspond to positive and negative isosurface values (±0.03), respectively. (For interpretation of the references to colour in this figure legend, the reader is referred to the web version of this article.)

The structures show that the aromatic **dpa** and **dipm** ligands are not planar. In particular for compound **C1** the dihedral angle between the two pyridyl rings is predicted to be 148.5°, which compares well with the experimental value of 147.6° [13]. This dihedral angle is calculated to be 142.8° in **C2**, 150.6° in **C3** and 148.7° in **C4**. The substitution of chlorides with ammine ligands subtly affects also the dihedral angle between the plane containing Pt and the monodentate ligands and the plane of the aromatic rings. This angle varies from about 152° in **C1** and **C3** to about 137° in **C2** and **C4**. These structural features may affect the interac-

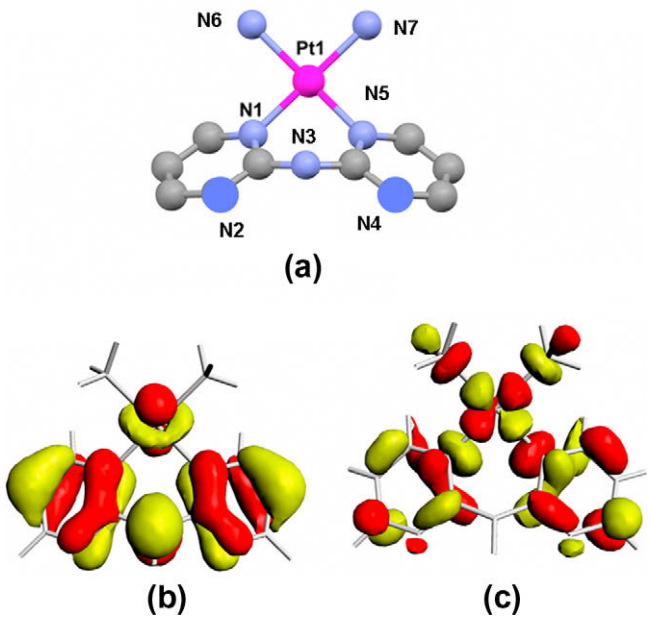

Fig. 6. Energy minimized structure of **C4** (a), (b) HOMO and (c) LUMO. The red (dark) and green (light) isosurfaces correspond to positive and negative isosurface values (±0.03), respectively. (For interpretation of the references to colour in this figure legend, the reader is referred to the web version of this article.)

Table 1
Comparison of geometric data for **C1** with the DFT calculation.

Experimental Bond lengths	(Å)	Calculated Bond lengths	(Å)
Pt–Cl1	2.301	Pt–Cl1	2.331
Pt–Cl2	2.292	Pt–Cl2	2.332
Pt–N1	2.010	Pt–N1	2.084
Pt–N2	2.012	Pt–N2	2.086
Bond angles	(°)	Bond angles	(°)
Cl–Pt–N	90.95	Cl–Pt–N	90.82
Cl–Pt–Cl	89.37	Cl–Pt–Cl	88.62
N–Pt–N	88.68	N–Pt–N	89.83

tion with the biological targets and ultimately the *in vitro* cytotoxicity, in addition to differences in chemical behavior, like solvolysis.

Compounds **C1** and **C3** have the same coordination sphere around the platinum i.e., two N-atoms and two chloride ions. Similarly, the other two compounds (**C2** and **C4**) have a four N-atom environment, two of which originate from monodentate ammine ligands and the other two are from the bidentate ligands. The HOMO and LUMO pictures are provided along with the optimized structures. As might have been expected, the HOMO and LUMO character remains the same when changing the ligand from **dpa** to **dipm**, but it is strongly modified by substituting Cl^- with NH_3. From the HOMO–LUMO pictures it is clear that in **C1** and **C3** the nonbonding electrons reside in the p-orbital of chlorides and they can also take part in pπ–dπ bonding, but there is no such situation for NH_3 ligands in **C2** and **C4**.

3.4. DNA model base studies with 9-EtG

The DNA model base 9-ethyl guanine is often used to follow the binding of metal compounds (e.g. platinum, ruthenium or gold) by NMR, or ESI-MS analytical techniques [34–39]. This simple molecule binds to metal compounds at N7 in a straightforward way to form kinetically stable adducts. Generally, the easily hydrolysable ligands are replaced by 9-EtG in a time scale which can be followed spectroscopically. The numbering scheme for the platinum compounds and 9-EtG is shown in Fig. 7. Compounds **C2** and **C4** were not involved in this reaction, given their kinetically inertness to ligand exchange.

The model base has been added in different molar equivalences to the platinum compound (**C1** and **C3**) and NMR spectra have been recorded within certain time intervals. In the presence of an excess of 9-EtG (1:4 M ratio of Pt:9-EtG) prominent changes starts appearing for both **C1** and **C3** after 45 min at 37 °C and the changes continue up to 18 h. The changes in the proton NMR spectra are shown in Figs. 8 and 10 and in Figs. 9 and 11 for a series of ^{195}Pt spectra. The spectra of the formed adducts remain the same when different amounts (1:1) of model base are used (data not shown). Different symbols have been used to differentiate between unreacted 9-EtG (♦), starting platinum compounds (**C1** or **C3**; ●) and the formed adducts with 9-EtG (■) in the serial spectra, respectively.

3.4.1. *C1* with 9-EtG

For **C1**, two different ratios of platinum compound to model base (1:1 and 1:4) have been studied at 37 °C (as physiological condition) in dmso-d_6. The presence of characteristic peaks from starting materials, **C1** and 9-EtG has revealed that the reaction is not complete after days. ^{195}Pt NMR also reveals the presence of three different species in the reaction mixture. Three peaks can be assigned as PtN_2Cl_2 (−2086 ppm) [40], PtN_3Cl (−2216 ppm) and PtN_2ClS (−2835 ppm) coordination sphere according to the database [23,41]. The gradual changes in the stacked spectra are depicted in Fig. 8.

After solvolysis of one of the chloride ligands the cationic species $[Pt(dpa)(dmso)Cl]^+$ with a PtN_2ClS coordination sphere appears to be formed (the same peak is also observed in dmso without the addition of 9EtG). The peak did not markedly increase or decrease in intensity up to 36 h. The third peak appearing at −2216 ppm, corresponds to Pt in a N_3Cl environment. This indicates that one of the chloride ligands has been replaced by 9-EtG, giving rise to the cation $[Pt(dpa)(9\text{-EtG})Cl]^+$, the monosubstituted adduct. The appearance of the three peaks (relative peak heights 1:5:2) was found to be independent on the used ratio of the model

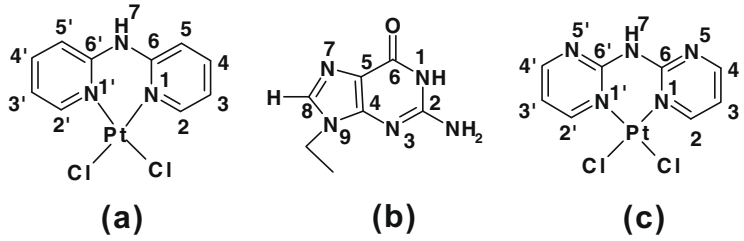

Fig. 7. Numbering scheme of the atoms for (a) **C1**, (b) 9-EtG and (c) **C3**.

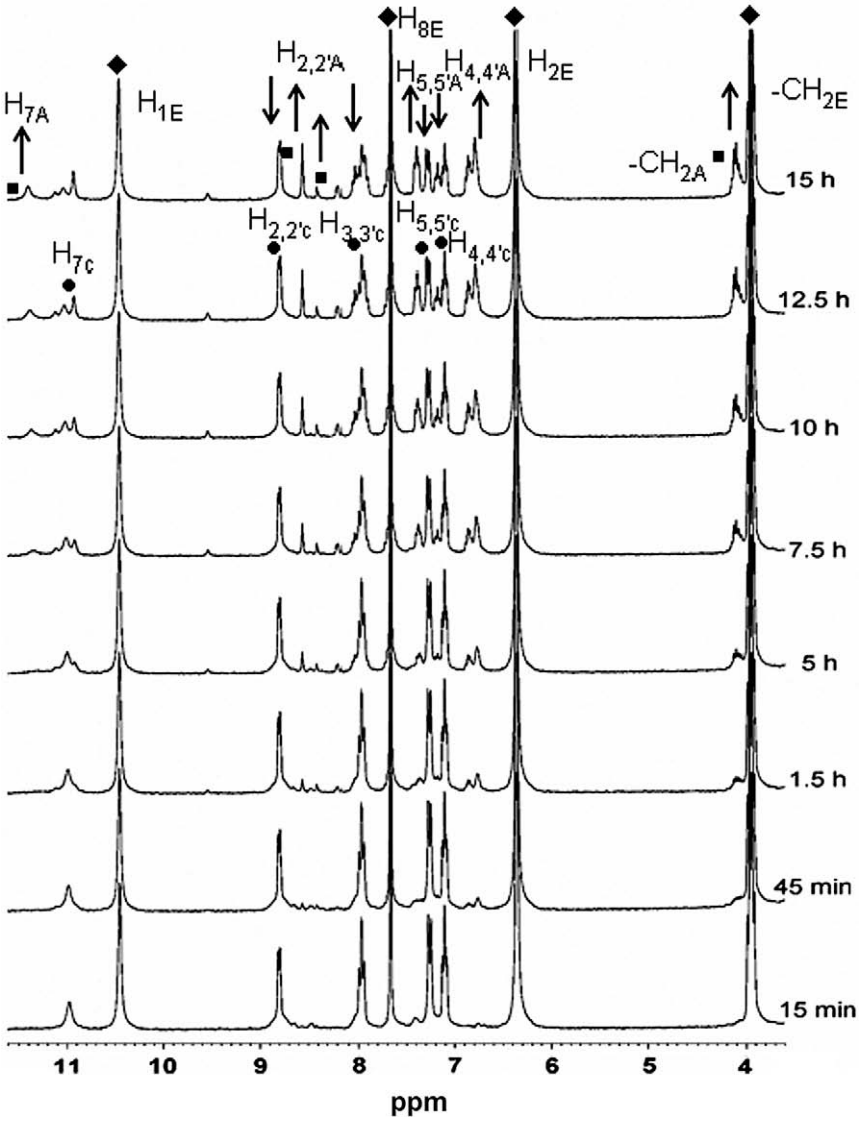

Fig. 8. Time-dependent changes in the ^{1}H NMR spectrum of **C1** upon addition of 4 equivalents of 9-ethylguanine (in dmso-d_6) with product marking, as unreacted and excess 9-EtG (♦), **C1** (●) and the **C1** adduct with 9-EtG (■).

base to the platinum compound during the observed reaction period. The presence of the three species was further supported by ESI-MS analysis of the reaction mixture, directly from NMR tubes.

*3.4.2. **C3** with 9-EtG*

The ^{1}H NMR spectra of **C3** with 4 equivalents of 9-EtG are shown in Fig. 10. After 45 min new peaks are appearing, confirming that a reaction is taking place between the platinum compound and 9-EtG. In theory the chloride ligands from the platinum compound may be solvolyzed by dmso, or substituted by 9-EtG. From the ^{195}Pt NMR spectra, shown in Fig. 11, changes can be observed with time. **C3** gives rise to a peak at −2048 ppm, corresponding to platinum in a N_2Cl_2 environment [22,23,40]. After 6 h, a new peak appears at −2835 ppm, which corresponds to platinum in a N_2ClS environment (from [Pt(dipm)(dmso)Cl]Cl species), *via* solvolysis [23,41]. The peak, surprisingly, appears not to increase or decrease in intensity over the observed time window (18 h). The third peak starts to appear at −2177 ppm, and corresponds to platinum in a N_3Cl environment (from [Pt(dipm)(9-EtG)Cl]Cl species *via* substitution). This clearly indicates that only one of the chloride ligands has been replaced by 9-EtG, giving rise to the monosubstituted adduct. The presence of the three different species has been confirmed by ESI-MS.

3.5. In vitro cytotoxicity

The 60- or 19-cell-line testing panels used and recommended by the National Cancer Institute (NCI, USA) [42–44] are quite exhaustive to evaluate cytotoxic activity of numerous new samples. Therefore, an easily manageable scaled-down 7-cell panel from different organ origins has been selected; this would provide the feasibility to test a wide range of samples in one cycle. The use of different solvents (dmso as used by NCI, or water) facilitates the activation of the compounds by different reaction solvolysis pathways, which might influence the activity *in vitro*. Short (48 h as used by NCI) or longer (96 h) incubation times may have an effect on the uptake and accumulation of the various compounds. Three clinically-approved platinum drugs along with some typical reference compounds have been tested under the same conditions for comparison purposes, and the results are described below.

The results of the cytotoxicity assays of the present four compounds are summarized in a tabular form. The results of platinum

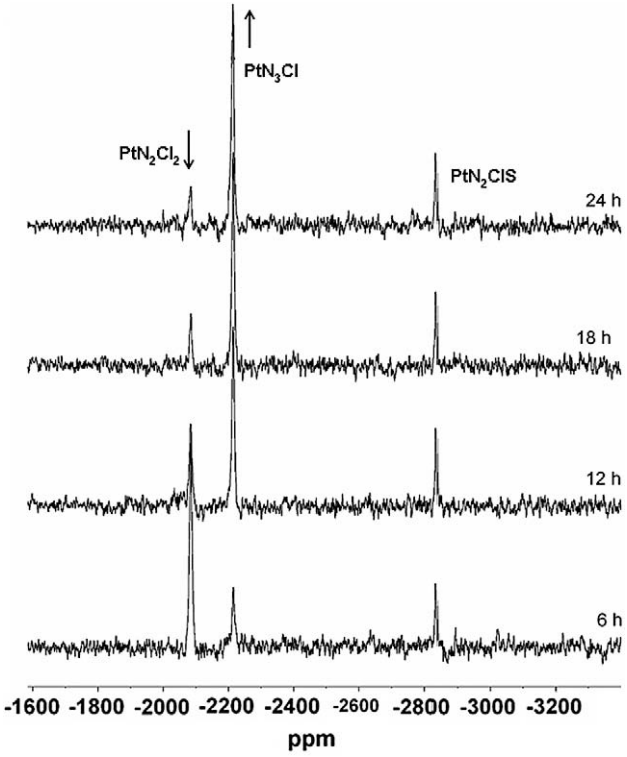

Fig. 9. Time-dependent changes in the ^{195}Pt NMR spectrum of **C1** upon addition of 4 equivalents of 9-EtG (in dmso-d_6) and the assignments of the peaks.

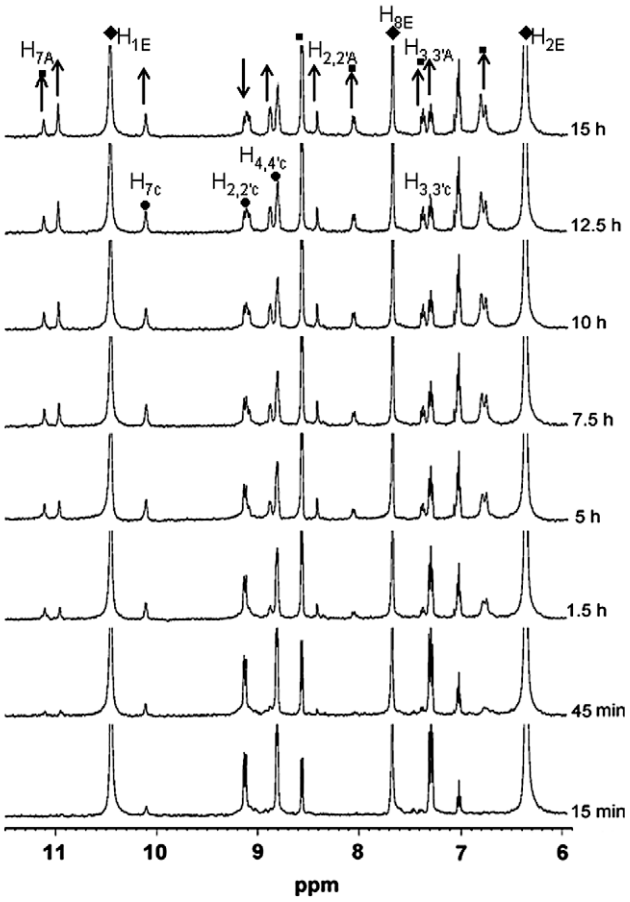

Fig. 10. Time-dependent changes in the ^{1}H NMR spectrum of **C3** upon addition of 4 equivalents of 9-EtG (in dmso-d_6) with product marking, as unreacted and excess 9-EtG (♦), **C3** (●) and the **C3** adduct with 9-EtG (■), respectively.

drugs for 120 h and 48 h incubation periods have been depicted in Tables 2 and 3, respectively. Each sample was tested for ten different concentrations (from freshly prepared 5 mg/mL dmso stock solutions) and in quadruplicate. The 48 h incubation time experiments were studied with freshly prepared samples from a stock in milliQ water (1 mg/mL) and investigated in the same cell lines as the 120 h experiments. These two parameters (time of incubation and stock concentration) have been changed in order to find out the effect of reversibility of DNA-Pt adduct as a function of the incubation period. For longer incubation time, the DNA-Pt adduct can get repaired easily whereas with shorter incubation time the repair mechanism has limited time. The change in stock concentration eventually affects the quantity of platinum compound in the cells. The direct relationship can not be predicted yet, however, the effect is shown in the results. The solvent used for tests are different, but the step-wise gradual dilution eliminates any possible effect of solvolysis during the experimental period.

The SRB assay [31], when performed under slightly different conditions than common practice, did lead to a significant observation. The most common experimental methods in the SRB assay involve incubation times of 120 h and a stock solution of 5 mg/mL in dmso (followed by subsequent dilution with medium). The reference compounds used generally are organic drugs (except cisplatin) with no structural similarity or mode of action. The cell lines used are seven human tumor cell lines with different origin and type.

In case of the platinum reference compounds the behavior is different. Oxaliplatin and [Pt(dach)Cl_2] are very active even with shorter exposure time, 48 h of incubation, in all used cell lines. The low IC_{50} values in all cases are less then 2 μM for these two compounds. On the other hand, carboplatin and cisplatin exhibit higher IC_{50} values compared to the organic or the other two platinum compounds (oxaliplatin and [Pt(dach)Cl_2]), which indicates a time-dependent cytotoxicity.

Under similar experimental condition (but longer incubation time of 120 h) the only active newly synthesized compound is **C3**. The inhibitory concentration is as high as 1.6-fold (H226) to 10-fold (M19-MEL), compared to cisplatin. In spite of similarity in the structure (there are two hydrolysable chloride groups on both of them, so a similar mode of action might be expected) of **C3** [Pt(dipm)Cl_2] with cisplatin, the activities towards cancer cell lines are quite different. The other cisplatin analogue with N_2Cl_2 coordination sphere, **C1**, [Pt(dpa)Cl_2] is active only in the EVSA-T cell line. The other two coordinatively saturated compounds, **C2** $[Pt(dpa)(NH_3)_2]^{2+}$ and **C4** $[Pt(dipm)(NH_3)_2]^{2+}$ are showing almost no activity in all used cell lines. These two compounds having 2+ charges would be expected to strongly interact with DNA at least by electrostatic attraction to phosphate backbone; the compounds in a way resemble those of formula $[Pt(en)(N–N)]^{2+}$ reported by Aldrich-Wright et al. which show selective antileukemic activity (L1210 cell line) [45–50].

When the incubation time is changed from 120 h to 48 h, the two highly water-soluble platinum compounds; **C2** and **C4** show enhanced activity (similar or better than cisplatin) especially in the EVSA-T cell lines. When compared with carboplatin, the activity increases up to 4- and 1.5-fold, respectively. In this experiment the stock solution is prepared in milliQ water, but absence of any easily hydrolysable ligand on the platinum centre nullifies the activation of sample (unlike the cisplatin activation *via* hydrolysis). The effect of shorter incubation time probably indicates the stability of DNA-platinum adduct. In this time-scale, the intercalated platinum moieties possibly render irreparable DNA damage. The

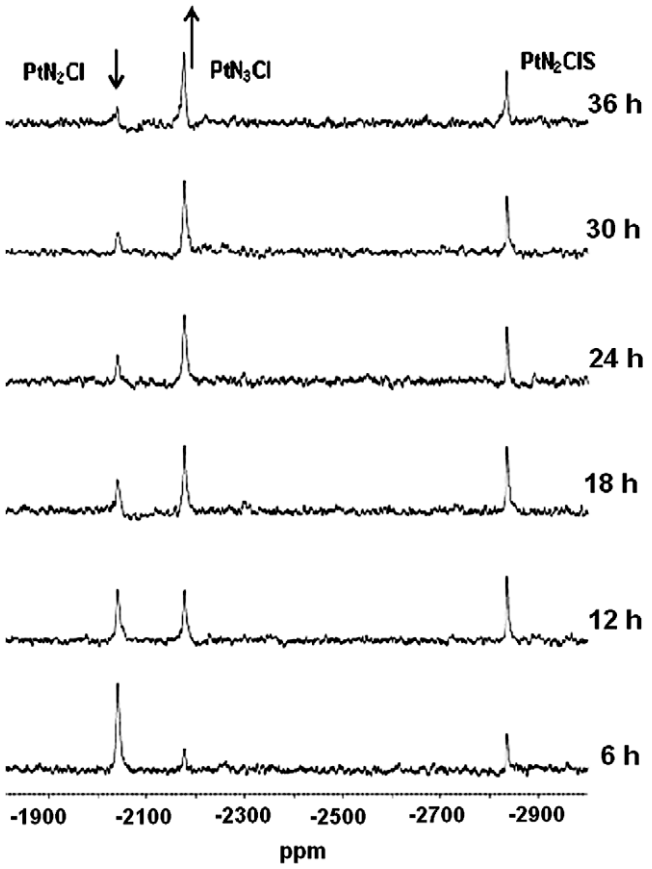

Fig. 11. Time-dependent changes (6–36 h) in the ^{195}Pt NMR spectrum of **C3** upon reaction with 4 equivalents of 9-EtG and the assignments of the peaks.

Table 2
IC_{50} values (μM) for the platinum compounds, cisplatin and **C1**–**C4** (120 h incubation).

Samples	Cell lines						
	A498	EVSA-T	H226	IGROV	M19-MEL	MCF-7	WIDR
Cisplatin	7.51	1.41	10.9	0.56	1.85	2.32	3.22
Carboplatin [53]	14.3	2.96	–	2.10	9.43	14.8	4.04
C1	74.2	16.7	62.6	62.6	47.7	60.3	52.8
C2	68.1	>100	64.5	>100	88.8	98.7	94.6
C3	17.1	6.33	17.8	19.4	18.6	12.1	19.2
C4	78.2	13.4	76.4	65.4	88.8	>100	>100

Table 3
IC_{50} values (μM) for **C2**, **C4** and four reference platinum compounds (48 h incubation).

Samples	Cell lines						
	A498	EVSA-T	H226	IGROV	M19-MEL	MCF-7	WIDR
C2	>100	17.2	>100	>100	>100	>100	>100
C4	>100	7.08	>100	71.2	>100	>100	>100
Cisplatin	8.22	17.7	10.7	2.94	10.3	17.1	22.0
Carboplatin	56.5	27.7	30.9	10.3	18.1	37.1	27.2
Oxaliplatin	0.054	0.44	0.64	1.49	0.90	0.54	0.65
[Pt(dach)Cl_2]	0.44	0.51	0.56	1.29	0.79	0.49	0.62

longer incubation time probably allows the adduct to disintegrate and repair the damage. Consequently no killing of the cell is observed. It has also been shown in the EVSA-T cell lines, that several gene-specific signaling pathways are active [51,52]. Therefore, the proper explanation of the enhanced and selective activity remains still uncertain, requiring further in-depth investigations.

4. Conclusions

In this study the successful synthesis and characterization of three new platinum compounds (**C2**, **C3** and **C4**) with reproduction and characterization of an earlier synthesized one (**C1**), are reported. The structures of all four coordination compounds have been energy-minimized using DFT calculations. This optimization confirms that all the compounds cannot be coplanar for metal and ligands, but be rather more organized in a puckered orientation. The bidentate ligands (**dpa** and **dipm**) induce a fold around the central–NH moiety of an open book structure.

The compounds with two chloride ligands, **C1** and **C3**, were reacted with the DNA model base, 9-ethylguanine in dmso solution. Both compounds react to form a monoadduct with 9-EtG. Despite the use of an excess of model base, no bisadduct appears to be formed, as is known in the case of cisplatin. Both the studied compounds undergo facile solvolysis by solvent (dmso) and the solvated cationic products are quite stable with easy detection (by NMR and ESI-MS). This solvated product formation process competes with the monoadduct or bisadduct formation processes. The bisadduct formation is feasible either *via* the second chloride dissociation (from PtN_3Cl species, monoadduct) or two-step reaction of PtN_2ClS (dissociation of chloride and dimethylsulfoxide followed by the substitution with two 9-ethylguanine molecules). None of the process could be detected as the peak height of PtN_3Cl increases and gets stabilized, whereas the peak height of PtN_2ClS appears to be unchanged.

The activity of **C3** towards selected cell lines is promising to balance toxicity and selectivity. The cationic compounds (**C2** and **C4**) are significantly active against EVSA-T cell lines, while inactive towards MCF-7 cell lines (both cell lines are breast cancer cells with difference in their hormone level). These compounds might be potential candidates for use in leukemic cell lines as the cationic $[Pt(en)(N–N)]^{2+}$ species exhibit significant activity in L1210 cell lines. All the compounds could bind to DNA as primary target, although the detailed cellular process requires further exploration. Modification of the ligands, chemically and sterically, might give further clues to this hypothesis. The attachment of a fluorescent tag or a receptor target with the amine N-atom of the ligand, would allow to follow the drug *in vitro* and also to target specific organs, respectively. In addition, the selective changes in the carrier ligand may modify the activity profile, the solubility and the bioavailability.

Acknowledgements

We are grateful to Pharmachemie, PCN, Haarlem (The Netherlands) for conducting the cytotoxicity tests. Johnson-Matthey (Reading, UK) is gratefully thanked for their generous loan scheme of K_2PtCl_4.

Appendix A. Supplementary material

Supplementary data associated with this article can be found, in the online version, at doi:10.1016/j.jinorgbio.2009.07.004.

References

[1] E.R. Jamieson, S.J. Lippard, Chem. Rev. 99 (1999) 2467–2498.
[2] L. Kelland, Nat. Rev. Cancer 7 (2007) 573–584.
[3] L. Kelland, Expert Opin. Investig. Drugs 16 (2007) 1009–1021.
[4] Y.W. Jung, S.J. Lippard, Chem. Rev. 107 (2007) 1387–1407.

[5] D. Wang, S.J. Lippard, Nat. Rev. Drug Discov. 4 (2005) 307–320.
[6] J. Reedijk, Proc. Nat. Acad. Sci. USA 100 (2003) 3611–3616.
[7] S. Roy, J.A. Westmaas, K.D. Hagen, G.P. van Wezel, J. Reedijk, 103 (2009) 1288–1297.
[8] V. Brabec, V. Kleinwachter, J.L. Butour, N.P. Johnson, Biophys. Chem. 35 (1990) 129–141.
[9] V. Brabec, Prog. Nucleic Acid Res. 71 (2002) 1–68.
[10] M.F. Brana, M. Cacho, A. Gradillas, B. de Pascual-Teresa, A. Ramos, Curr. Pharm. Des. 7 (2001) 1745–1780.
[11] W.B. Yao, K. Kavallieratos, S. de Gala, R.H. Crabtree, Inorg. Chim. Acta 311 (2000) 45–49.
[12] D.C. Li, D.J. Liu, Cryst. Res. Technol. 39 (2004) 359–362.
[13] C. Tu, X.F. Wu, Q. Liu, X.Y. Wang, Q. Xu, Z.J. Guo, Inorg. Chim. Acta 357 (2004) 95–102.
[14] M.J. Rauterkus, S. Fakih, C. Mock, I. Puscasu, B. Krebs, Inorg. Chim. Acta 350 (2003) 355–365.
[15] G.A. van Albada, I. Mutikainen, U. Turpeinen, J. Reedijk, Inorg. Chem. Commun. 9 (2006) 1067–1070.
[16] G.A. van Albada, I. Mutikainen, U. Turpeinen, J. Reedijk, J. Mol. Struct. 837 (2007) 43–47.
[17] S. Roy, J.A. Westmaas, F. Buda, J. Reedijk, J. Inorg. Biochem. (2009), doi:10.1016/j.jinorgbio.2009.07.003.
[18] S.C. Dhara, Ind. J. Chem. 8 (1970) 193–196.
[19] J. Price, R. Schramm, B. Wayland, A. Williams, Inorg. Chem. 11 (1972) 1280–1284.
[20] M. Brown, in: WIN Plot : Simple and Easy Plotting, 2006.
[21] L.V. Interrante, R.P. Messmer, Inorg. Chem. 10 (1971) 1174–1178.
[22] J.R.L. Priqueler, I.S. Butler, F.D. Rochon, Appl. Spectrosc. Rev. 41 (2006) 185–226.
[23] B.M. Still, P.G.A. Kumar, J.R. Aldrich-Wright, W.S. Price, Chem. Soc. Rev. 36 (2007) 665–686.
[24] ADF2007.01, in: ADF2007.01, SCM, Theoretical Chemistry, Vrije Universiteit, Amsterdam, The Netherlands, <http://www.scm.com>.
[25] C.F. Guerra, J.G. Snijders, G. te Velde, E.J. Baerends, Theor. Chem. Acc. 99 (1998) 391–403.
[26] G.T. Velde, F.M. Bickelhaupt, E.J. Baerends, C.F. Guerra, S.J.A. Van Gisbergen, J.G. Snijders, T. Ziegler, J. Comput. Chem. 22 (2001) 931–967.
[27] A.D. Becke, Phys. Rev. A 38 (1988) 3098–3100.
[28] C.T. Lee, W.T. Yang, R.G. Parr, Phys. Rev. B 37 (1988) 785–789.
[29] E. van Lenthe, A. Ehlers, E.J. Baerends, J. Chem. Phys. 110 (1999) 8943–8953.
[30] A.T.M. Marcelis, C. Erkelens, J. Reedijk, Inorg. Chim. Acta 91 (1984) 129.
[31] Y.P. Keepers, P.E. Pizao, G.J. Peters, J. Vanarkotte, B. Winograd, H.M. Pinedo, Eur. J. Cancer 27 (1991) 897–900.
[32] C.V. Diaconu, A.E. Cho, J.D. Doll, D.L. Freeman, J. Chem. Phys. 121 (2004) 10026–10040.
[33] R.K. Hocking, R.J. Deeth, T.W. Hambley, Inorg. Chem. 46 (2007) 8238–8244.
[34] K. Aoki, M.A. Salam, C. Munakata, I. Fujisawa, Inorg. Chim. Acta 360 (2007) 3658–3670.
[35] A. Garza-Ortiz, P.U. Maheswari, M. Siegler, A.L. Spek, J. Reedijk, Inorg. Chem. 47 (2008) 6964–6973.
[36] G. Kampf, M. Willermann, E. Freisinger, B. Lippert, Inorg. Chim. Acta 330 (2002) 179–188.
[37] S. Komeda, M. Lutz, A.L. Spek, Y. Yamanaka, T. Sato, M. Chikuma, J. Reedijk, J. Am. Chem. Soc. 124 (2002) 4738–4746.
[38] A.F.A. Peacock, A. Habtemariam, R. Fernandez, V. Walland, F.P.A. Fabbiani, S. Parsons, R.E. Aird, D.I. Jodrell, P.J. Sadler, J. Am. Chem. Soc. 128 (2006) 1739–1748.
[39] E. Corral, A.C.G. Hotze, A. Magistrato, J. Reedijk, Inorg. Chem. 46 (2007) 6715–6722.
[40] I. Lakomska, E. Szlyk, J. Sitkowski, L. Kozerski, J. Wietrzyk, M. Pelczynska, A. Nasulewicz, A. Opolski, J. Inorg. Biochem. 98 (2004) 167–172.
[41] S.J. Berners-Price, L. Ronconi, P.J. Sadler, Prog. Nucl. Magn. Reson. Spectrosc. 49 (2006) 65–98.
[42] M. Alvarez, R. Robey, V. Sandor, K. Nishiyama, Y. Matsumoto, K. Paull, S. Bates, T. Fojo, Mol. Pharmacol. 54 (1998) 802–814.
[43] K. Bracht, Boubakari, R. Grunert, P.J. Bednarski, Anti-Cancer Drugs 17 (2006) 41–51.
[44] K. Bracht, M. Liebeke, C.A. Ritter, R. Grunert, P.J. Bednarski, Anti-Cancer Drugs 18 (2007) 389–404.
[45] C.R. Brodie, J.G. Collins, J.R. Aldrich-Wright, Dalton Trans. (2004) 1145–1152.
[46] D.M. Fisher, P.J. Bednarski, R. Grunert, P. Turner, R.R. Fenton, J.R. Aldrich-Wright, ChemMedChem 2 (2007) 488–495.
[47] D. Jaramillo, D.P. Buck, J.G. Collins, R.R. Fenton, F.H. Stootman, N.J. Wheate, J.R. Aldrich-Wright, Eur. J. Inorg. Chem. (2006) 839–849.
[48] D. Jaramillo, J.G. Collins, P. Junk, J.R. Aldrich-Wright, J. Inorg. Biochem. 96 (2003) 159.
[49] S. Kemp, N.J. Wheate, D.P. Buck, M. Nikac, J.G. Collins, J.R. Aldrich-Wright, J. Inorg. Biochem. 101 (2007) 1049–1058.
[50] N.J. Wheate, C.R. Brodie, J.G. Collins, S. Kemp, J.R. Aldrich-Wright, Mini-Rev. Med. Chem. 7 (2007) 627–648.
[51] M. Wasielewski, F. Elstrodt, J.G.M. Klijn, E. Berns, M. Schutte, Breast Cancer Res. Tr. 99 (2006) 97–101.
[52] A. Hollestelle, F. Elstrodt, J.H.A. Nagel, W.W. Kallemeijn, M. Schutte, Mol. Cancer Res. 5 (2007) 195–201.
[53] M. Gielen, R. Willem, A. Bouhdid, D.D. Vos, in, Dibutyltin bis(dihydroxybenzoates) and Compositions Containing these Compounds, Pharmachemie B.V. (Haarlem, NL), United States, 1996.